



The influence of the transformation of electronic structure and microstructure on improving the thermoelectric properties of zinc antimonide thin films



Zhuang-hao Zheng^{a,b}, Ping Fan^{a,b,*}, Jing-ting Luo^{a,b}, Peng-juan Liu^a, Xing-min Cai^a, Guang-xing Liang^{a,b}, Dong-ping Zhang^a, Ye Fan^a

^a College of Physics Science and Technology, Institute of Thin Film Physics and Applications, Shenzhen University, 518060, China

^b Shenzhen Key Laboratory of Sensor Technology, Shenzhen University, 518060, China

ARTICLE INFO

Article history:

Received 16 December 2014

Received in revised form

16 April 2015

Accepted 16 April 2015

Available online

Keywords:

A. Thin films and multilayers

B. Electronic structure

B. Thermoelectric properties

ABSTRACT

Measurements of electronic structure, microstructure and thermoelectric properties of zinc antimonide thin films prepared by direct current magnetron co-sputtering were carried out. The as-deposited zinc antimonide thin film had a very high resistivity similar to insulating ceramics, which was due to a low binding energy of both zinc and antimony, with the electron scattering increases and impedes the current transport. With the increase in annealing temperature, the films became more crystalline and the thermoelectric properties were also improved. The resistivity of the film decreased rapidly with its crystallinity when the annealing temperature was above 350 °C. The Seebeck coefficients of the thin films were positive, indicating that the films were P-type. The Seebeck coefficient of those samples increased with increasing annealing temperature. The thin film annealed at 400 °C has an optimal power factor of $1.87 \times 10^{-3} \text{ Wm}^{-1} \text{ K}^{-2}$ with a Seebeck coefficient of $300 \mu\text{VK}^{-1}$ and a resistivity of $4.82 \times 10^{-5} \Omega\text{m}$ at 573 K.

© 2015 Elsevier Ltd. All rights reserved.

1. Introduction

Thermoelectric materials with high conversion efficiency for possible applications in energy conversion have attracted much attention in recent years [1]. The performance of thermoelectric materials is determined by the dimensionless figure of merit (ZT) which is defined as $S^2T/\rho\kappa$, where S is the Seebeck coefficient, T is the absolute temperature, ρ is the resistivity and κ is the thermal conductivity [2]. Zinc antimonide (Zn–Sb) binary system is one of the promising P-type thermoelectric materials for low cost thermoelectric application [3–5]. The ZT of Zn–Sb based bulk compound is reported to be 1.3 [6]. However, its thermoelectric properties are still inadequate for practical use compared with other thermoelectric materials [7,8]. Thin film technique is one of the methods for improving the thermoelectric properties of thermoelectric material due to the stronger quantum confinement

effect with low dimensional structure materials [9–11]. For instance, a high room-temperature ZT value of 2.4 has been reported for P-type superlattices thin films [12]. Besides, thin film thermoelectric material has a huge potential application in miniaturized sensors and micropower source, etc [13–15].

Several techniques [16,17] have been used to grow Zn–Sb based thin films. Sun et al. [18] fabricated high-performance Zn–Sb based thin films by sputtering. The ZT at 573 K is estimated to be 1.15 by using bulk thermal conductivity from their data [18]. In many cases, the thermal conductivity of thin film is much lower than that of the corresponding bulk materials [19,20], indicating that the ZT of the Zn–Sb based thin films prepared by Sun is much higher than 1.15. Their results show that Zn–Sb thin film is promising for thermoelectric applications. Although several techniques have been used to grow Zn–Sb based thin films, it is still rarely reported in practice. Much work is needed in preparing high-performance zinc antimonide thin film.

Zn–Sb based thin films were deposited by direct current (DC) magnetron co-sputtering in this work. The influence of post-annealing temperature on the electronic structure, microstructure and the thermoelectric properties of the thin films were

* Corresponding author. College of Physics Science and Technology, Institute of Thin Film Physics and Applications, Shenzhen University, 518060, China. Tel./fax: +86 755 26536021.

E-mail address: fanping308@126.com (P. Fan).

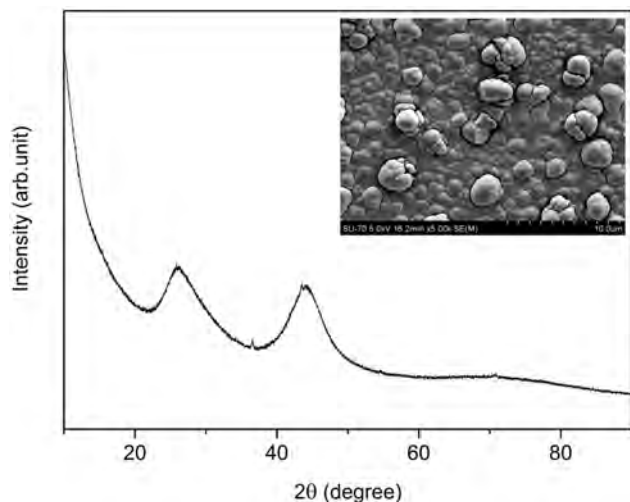


Fig. 1. XRD pattern and surface morphology of as-deposited Zn–Sb based thin film.

investigated. Besides, it is worth noting that the binding energy of Zn in the thin film was much lower than that of Zn in bulk material [21] and it may cause a great change of the electrical property. Therefore, the electronic structure of the thin films was also investigated.

2. Experimental details

Zn–Sb thin films were deposited at room temperature by co-sputtering. High purity (4N) Zn and Sb targets were used in a DC magnetron sputtering facility with a sputtering angle of 45° and a target–substrate distance of 10 cm. BK7 glass substrates were ultrasonically cleaned in acetone and alcohol for 10 min successively. The chamber was pumped down to a pressure less than 6.0×10^{-4} Pa prior to deposition. The working pressure was 0.4 Pa with Ar of 40 sccm as the sputtering gas. A 3-min pre-cleaning process was performed to remove contaminants on the surface of the targets before thin film deposition. The sputtering power for Zn and Sb was 40 W and 24 W respectively. The as-deposited thin films were annealed for 1 h at 300 °C, 350 °C, 400 °C and 450 °C, respectively, under Ar atmosphere with an annealing pressure of 440 Pa. The as-deposited thin films were named as T1, and those annealed at 300 °C, 350 °C, 400 °C and 450 °C were named as T2, T3, T4 and T5, respectively.

The surface morphology and composition of the thin films were obtained by scanning electron microscopy (SEM, S-4700) with an energy dispersive X-ray microanalysis system and atomic force microscope (AFM, CSPM5500). X-ray photoelectron spectroscopy (XPS) with Al K_{α} (Axis Ultra) was used to investigate the electronic structure of the thin films. The structure of the thin films was characterized by X-Ray diffraction (XRD) technique (Bruker-D8-Advance) in the conventional θ - 2θ mode with the Cu K_{α} radiation of

0.15406 nm. The thermoelectric properties of the thin films at various testing temperature were measured using the four-probe technique and Seebeck coefficient measurement system (SDFP-I) with the temperature gradient method at temperatures from 300 K to 573 K. The temperature difference between the cold and hot side was 20 K. The thickness of the samples was obtained by characterizing the cross sectional area of the thin film with SEM.

3. Results and discussions

Fig. 1 shows the XRD pattern of the as-deposited thin film (named as T1) with the inset showing its surface morphology. It is difficult to obtain the real crystal structure of T1 due to the wide main diffraction peaks. It can be found that T1 has an amorphous phase from the XRD pattern. Since the thin film was deposited at room-temperature and Zn is easy to form clusters [22], the big humps on the surface of T1 are very likely metallic Zn clusters. From the XRD and surface morphology analyses, T1 might be made of Zn and Sb mixed metal phase. The thermoelectric properties and composition of T1 is listed in Table 1. It can be found that T1 has a very high resistivity and its Seebeck coefficient was not obtained due to the huge resistivity.

The thermoelectric properties and compositions of the annealed samples are also shown in Table 1. It can be found that the compositions of T1 ~ T5 are similar. Though T2 has better electrical property than T1, it still has a huge resistivity and the Seebeck coefficient was not obtained neither. The resistivity of the thin films decreases with the increasing annealing temperature and the resistivity of T3 ~ T5 are much lower than that of T1 ~ T2. The Seebeck coefficient of T3–T5 was measured to be $181 \mu\text{VK}^{-1}$, $172 \mu\text{VK}^{-1}$ and $130 \mu\text{VK}^{-1}$ at room-temperature. The results indicate that the thin films annealed at 350, 400, 450 °C have much better thermoelectric properties than that of as-deposited sample.

Fig. 2 shows the XRD patterns of the annealed thin films. From Fig. 2, it can be found that T2 has poor crystallinity. The highest peak located at 27.2° in T2 is from the diffraction of ZnSb (231) plane [23,24]. Compared with T2, T3 has better crystallinity and it can be confirmed that T3 is made of compounds. The three major diffraction peaks located at $\sim 28.7^\circ$, $\sim 29.3^\circ$ and 33.0° of T3 are due to the diffraction from ZnSb (112), (121) and (211) plane [23,24]. Other strong peaks observed from T3 are also related to the ZnSb phase. Besides, few extra diffraction peak is observed from T3, indicating T3 has a single phase of ZnSb. The XRD patterns of T4 and T5 are very similar to that of T3, which implies that the phase of ZnSb is also dominant in T4 and T5. Though a few weak peaks related to the Sb plane and Zn_4Sb_3 plane can be observed from T5, the intensity is much smaller than the major ZnSb diffraction peaks and the ZnSb is still the dominant phase in T5. From the XRD results shown in Figs. 1 and 2, it can be concluded that the as-deposited thin film is almost amorphous. The crystallinity of the thin films improves and the thin films are transformed to be ZnSb phase which is almost the dominant phase when the annealing temperature was above 350 °C.

Table 1

The thermoelectric properties, thickness and composition of as-deposited and annealed thin films.

| Sample | Annealing temperature (°C) | Thickness (nm) | Resistivity ($\times 10^{-5} \Omega\text{m}$) | Room-temperature Seebeck coefficient (μVK^{-1}) | Composition | |
|--------|----------------------------|----------------|---|--|-------------|--------|
| | | | | | Zn (%) | Sb (%) |
| T1 | As-deposited | 714 | >50,000 | Immeasurability | 61.1 | 38.9 |
| T2 | 300 | 700 | >10,000 | Immeasurability | 57.2 | 42.8 |
| T3 | 350 | 659 | 14.3 | 181 | 59.3 | 40.7 |
| T4 | 400 | 654 | 12.9 | 172 | 59.7 | 40.3 |
| T5 | 450 | 632 | 9.5 | 130 | 60.9 | 39.1 |

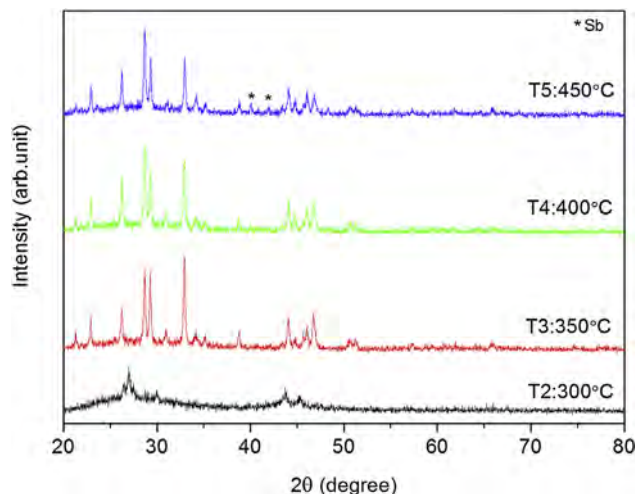


Fig. 2. XRD patterns of annealed Zn–Sb based thin films.

The AFM images of T2 ~ T5 are shown in Fig. 3. Though there are some humps on the surface of T2 which was annealed at 300 °C, the image is relatively smooth, this result implies that the grains are tiny and nearly non-crystalline. Some big humps can be observed in T3 which was annealed at 350 °C. But the humps are still discrete and the crystallinity grains are hard to recognize. The crystallinity grains of T4 become distinct and continuous when the annealing temperature was 400 °C, indicating that T4 has better crystallinity than T2 and T3. The grain size of T5 annealed at 450 °C is much larger than others. From the XRD and AFM analysis, the grain size is found to be enhanced with the increase in the annealing temperature. This suggests that the diffusion and mobility of the atoms are improved during the annealing process which leads to an improve

of the thin films crystallinity. The improved crystallinity and grain size can reduce the grain boundary scattering which favors the thermoelectric properties.

Though the crystallinity is one of the reasons that enhance the thin film thermoelectric properties, it is still very difficult to explain that the as-deposited thin film composed of Zn and Sb are almost insulative while the samples annealed over 300 °C is conductive. So the analysis of the electronic structure of all the thin films by XPS is necessary, as showing in Fig. 4. The C 1s peak at 284.88 eV from the surface or chamber contamination is used as an energy reference. The data extracted from Fig. 4 are listed in Table 2. The XPS instrumental error is 0.1–0.2 eV per peak position and the binding energy of Zn 2p peak and Sb 3d peak is totally different from the XPS results of ZnSb, Sb and Zn bulk materials [25,26]. The binding energy of Zn 2p peak of all the thin films is smaller than those of metallic Zn bulk materials and ZnSb. The binding energy of Sb 3d peak of T1 and T2 is also smaller than those of metallic Sb bulk materials. It can be considered that the T1 and T2 are easier to lose the electron in the form of thin film than that of metallic Sb bulk materials as Zn. It suggests that both of Zn and Sb are mainly as the free state, distributing in the thin film due to the deficient energy that cannot make the free electric electrons from outer Zn and Sb to form chemical bonds when the thin film deposited at low temperature. The disunity free electric electrons will be scattered or annihilated each other and impede the electric transport which causes the huge resistivity. There are three strong peaks observed from T3 in Fig. 4(a) which is exceptional. The great change of chemical shift is mainly due to that the thin film have two entirely different electronic structure from any other Sb based compound. When the annealing temperature was 400 °C, only the peak of Sb 3d_{5/2} was observed, revealing the thin film has a stable electronic structure. With the increase of the annealing temperature, the binding energy increases due to the deeper combination of the atomic. As shows in Fig. 4(b), the chemical shift of Zn 2p peak tends

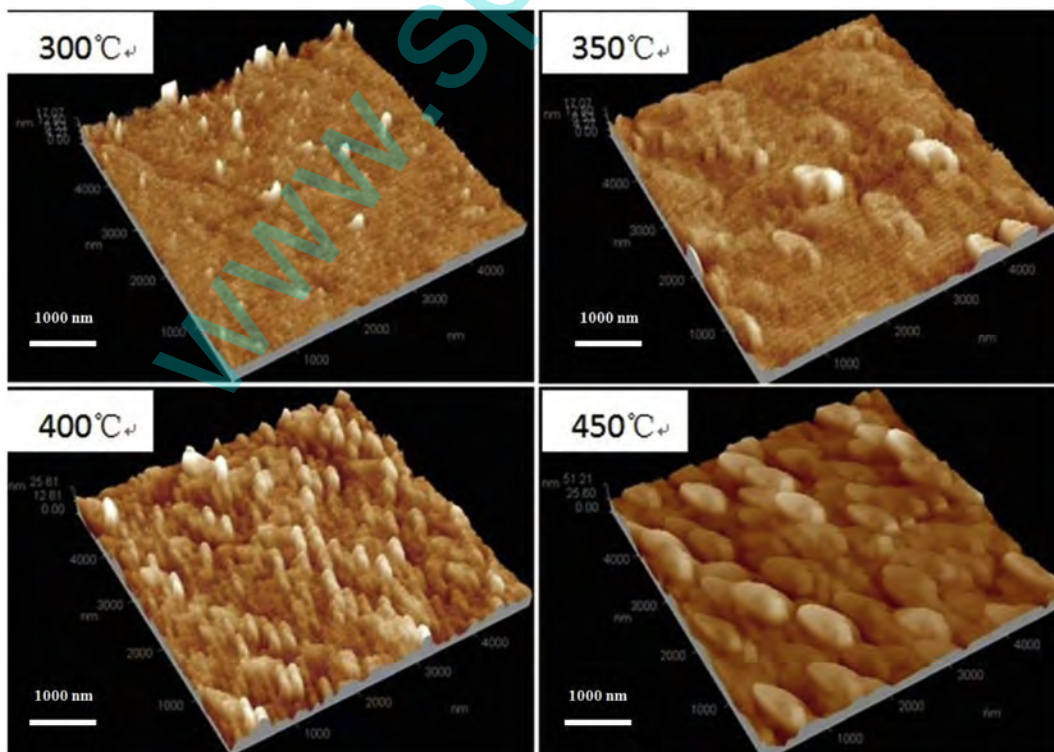


Fig. 3. AFM images of annealed Zn–Sb based thin films.

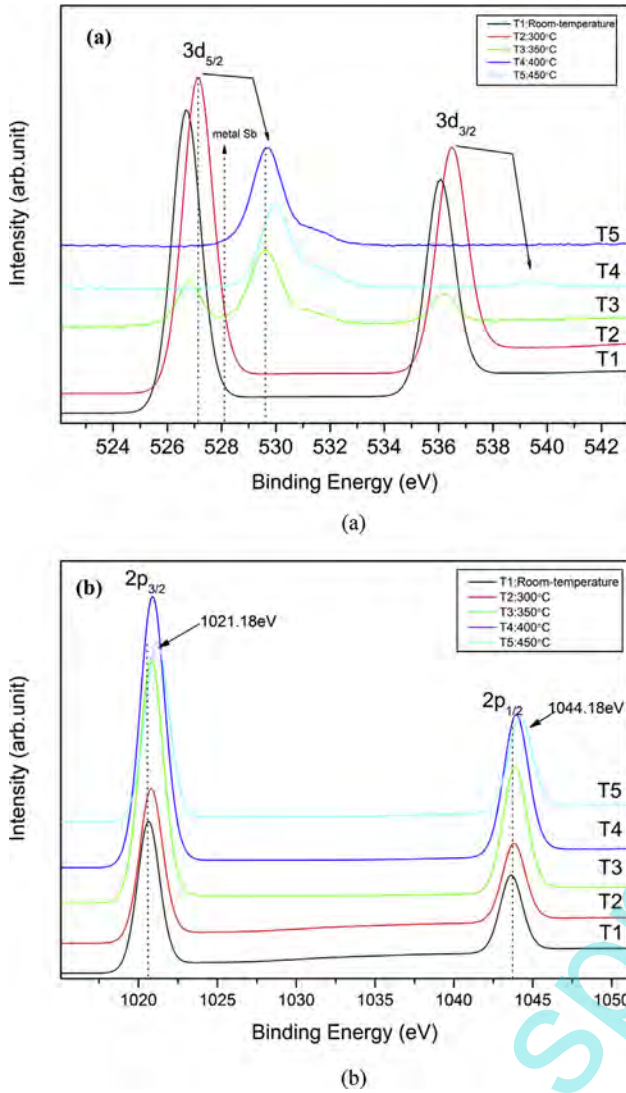


Fig. 4. XPS survey scans of the as-deposited and annealed thin films. (a) Sb 3d, (b) Zn 2p.

to increase with the increasing of the annealing temperature, which implies that Zn tends to catch electrons. The Zn binding energy becomes more and more close to the value of ZnSb bulk material, which confirms that the thin film has almost the same electronic structure with ZnSb. But they are still smaller than that of ZnSb bulk material, indicating that the Zn is easy to separate as free state electron which is good for decrease the thermal conductivity [27,28]. This is maybe one of the reason that why the thin film has lower thermal conductivity than bulk materials.

It was reported that Zn–Sb materials have nice thermoelectric properties above room-temperature [29]. The electrical and

Table 2

The binding energy of Sb 3d and Zn 2p of the as-deposited thin films, the annealed thin films, Zn, Sb and ZnSb bulk material.

| Sample | Sb 2d _{5/2} (eV) | Sb 2d _{3/2} (eV) | Zn 2p _{3/2} (eV) | Zn 2p _{1/2} (eV) |
|------------------|---------------------------|---------------------------|---------------------------|---------------------------|
| T1 | 526.68 | 536.08 | 1020.68 | 1043.68 |
| T2 | 527.08 | 536.48 | 1020.78 | 1043.78 |
| T3 | 526.78/529.58 | 536.18 | 1020.88 | 1043.88 |
| T4 | 529.68 | – | 1020.88 | 1043.88 |
| T5 | 529.98 | 539.68 | 1021.18 | 1044.18 |
| Sb [25] | 528.3 | 537.6 | – | – |
| Zn [25] | – | – | 1021.8 | 1044.8 |
| ZnSb [Ref. [26]] | – | – | 1021.3 | 1044.3 |

thermoelectric transport properties of T3 ~ T5 were measured at the temperature range of 300 K to 573 K and are shown in Fig. 5. In Fig. 5(a), the resistivity of T3~T5 decreases with the increase in the temperature, which reveals basically a semiconductor-like behavior. The minimal resistivity of $4.70 \times 10^{-5} \Omega\text{m}$ can be obtained from T5 at 573 K. Though the resistivity of T4 is higher than

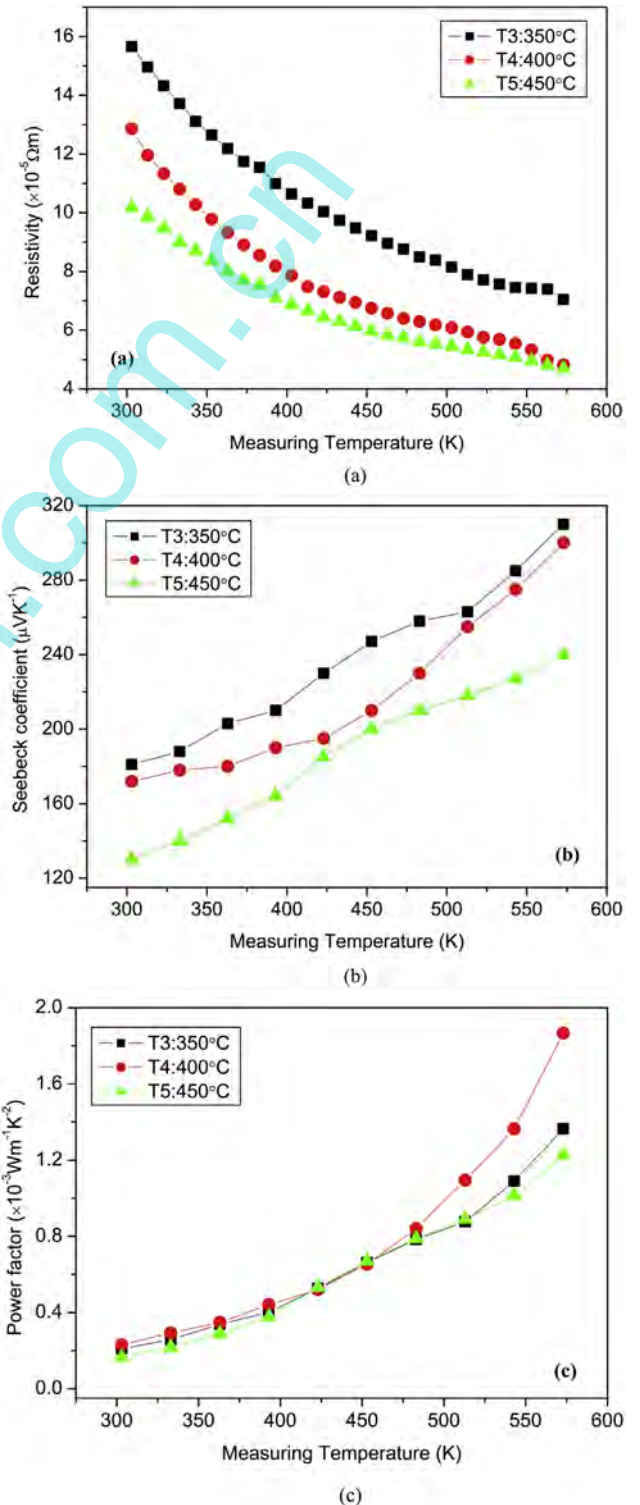


Fig. 5. Temperature dependence of the resistivity (a), Seebeck coefficient (b) and Power Factors (c) of the thin films annealed at 350 °C, 400 °C and 450 °C.

T5 at room-temperature, it decreases rapidly when the measuring temperature increases and have a value of $4.82 \times 10^{-5} \Omega\text{m}$ which is very close to that of T3. The better electric properties of T4 and T5 are mainly due to the more stable electronic structure and micro-structure. In Fig. 5(b), the positive Seebeck coefficients indicate that all the thin films are P-type. The entire Seebeck coefficient of the samples increases with the temperature increasing. The Seebeck coefficient of T3 has the largest value of $181 \mu\text{VK}^{-1}$ at room-temperature and increases to $310 \mu\text{VK}^{-1}$ at 573 K. This is probably due to the higher scattering of carriers which leads to an increase in Seebeck coefficient. The Seebeck coefficient of T4 is smaller than that of T3 at room-temperature and it increases rapidly to $300 \mu\text{VK}^{-1}$ when the measuring temperature increased to 573 K. T5 has a small Seebeck coefficient of $120 \mu\text{VK}^{-1}$ at 300 K and increases to $240 \mu\text{VK}^{-1}$ at 573 K. The power factor (PF), one of the important thermoelectric parameters, which determines the thermoelectric energy conversion, is defined as $S^2\sigma$ and has been shown in Fig. 5(c). The power factors of the thin films is very close when the measuring temperature is lower than 500 K indicating that the thin films have similar thermoelectric properties with similar micro-structure. However, the power factor of T4 is enhanced greatly when the testing temperature increases to above 500 K. T4 has an optimal power factor of $1.87 \text{ W m}^{-1} \text{ K}^{-2}$ with a Seebeck coefficient of $300 \mu\text{VK}^{-1}$ and a resistivity of $4.82 \times 10^{-5} \Omega\text{m}$ at 573 K. The result is excellent compared with the best results of the same material prepared by other technologies [16,18].

4. Conclusions

Zn–Sb based thin films were prepared by DC magnetron co-deposition at room temperature. The heat treatment under Ar atmosphere had been used to improve the performance of the thin films. The influence of annealing temperature on the electronic structure, micro-structure and thermoelectric properties of the thin films are investigated. The lower binding energy of both Zn 2p and Sb 3d of the thin film deposited at room temperature causes the huge resistivity of the sample. With the increase of annealing temperature, the binding energy increases and the thin film has the same electronic structure with ZnSb. After annealing over 300 °C, the crystallinity and grain size of the thin films improve and the thin films have a dominant phase of ZnSb. The thermoelectric properties of the thin films are also enhanced after annealing.

Acknowledgments

Supported by Special Project on the Integration of Industry, Education and Research of Guangdong Province (2012B091000174), Basical Research Program of Shenzhen (JCYJ20140418181958500) and Natural Science Foundation of SZU (grant no. 201418).

References

- [1] Snyder GJ, Toberer ES. *Nat Mater* 2008;7:105–14.
- [2] Zhao LD, Lo Sh, Zhang Y, Sun H, Tan G, Uher C, et al. *Nature* 2014;508:373–7.
- [3] Bjerg L, Madsen GK, Iversen BB. *Chem Mater* 2011;23:3907–14.
- [4] Rauwel P, Løvvik OM, Rauwel E, Taftø J. *Acta Mater* 2011;59:5266–75.
- [5] Lin JP, Qiao GJ, Ma LZ, Ren Y, Yang BF, Fei YJ, et al. *Appl Phys Lett* 2013;102:163902.
- [6] Snyder GJ, Christensen M, Nishibori E, Caillat T, Iversen BB. *Nat Mater* 2004;3:458–63.
- [7] Poudel B, Hao Q, Ma Y, Lan YC, Minnich A, Yu B, et al. *Science* 2008;320:634–8.
- [8] Shi X, Yang J, Salvador JR, Chi MF, Cho JY, Wang H, et al. *J Am Chem Soc* 2011;133:7837.
- [9] Hicks LD, Dresselhaus MS. *Phys Rev B* 1993;47:16631.
- [10] Hicks LD, Dresselhaus MS. *Phys Rev B* 1993;47:12727.
- [11] Valachová J, Zeipl R, Zelinka J, Malina V, Pavelka M, Jelínek M, et al. *Appl Phys Lett* 2005;87:081902.
- [12] Venkatasubramanian R, Siivola E, Colpitts T, O'Quinn B. *Nature* 2001;413:597.
- [13] Heremans JP, Jovovic V, Toberer ES, Saramat A, Kurosaki K, Charoenphakdee A, et al. *Science* 2008;321:554–7.
- [14] Fan P, Zheng ZH, Cai ZK, Chen TB, Liu PJ, Cai XM, et al. *Appl Phys Lett* 2013;102:033904.
- [15] Lee HB, Yang HJ, We JH, Kim K, Choi KC, Cho BJ. *J Electro Mater* 2011;40:615–9.
- [16] Zhang LT, Tsutsui M, Ito K, Yamaguchi M. *Thin Solid Films* 2003;443:84–90.
- [17] Lee HB, We JH, Yang HJ, Kim K, Choi KC, Cho BJ. *Thin Solid Films* 2011;519:5441–3.
- [18] Sun Y, Christensen M, Johnsen S, Nong NV, Ma Y, Sillassen M, et al. *Adv Mater* 2012;24:1693–6.
- [19] Dresselhaus MS, Chen G, Tang MY, Yang RG, Lee H, Wang DZ, et al. *Adv Mater* 2007;19:1043–53.
- [20] Hong JE, Lee SK, S.G Yoon. *J Alloy Comp* 2014;583:111–5.
- [21] Zheng ZH, Fan P, Liu PJ, Luo JT, Cai XM, Liang GX, et al. *Appl Surf Sci* 2014;292:823–7.
- [22] Spanhel L, Anderson MA. *J Am Chem Soc* 1991;113:2826–33.
- [23] JCPDS file No. 37–1008.
- [24] JCPDS file No. 05–0714.
- [25] Moulder JF, Chastain J. *Handbook of X-ray photoelectron spectroscopy*. 1995.
- [26] Böttger PH, Diplas S, Espen FL, Prytz Ø, Finstad TG. *J Phys Condens Matter* 2011;23:265502.
- [27] Li GD, Li Y, Liu LS, Zhang QJ, Zhai PC. *Mater Lett* 2013;107:348–50.
- [28] Schweika W, Hermann RP, Präger M, Perßon J, Keppens V. *Phys Rev B* 2007;99:125501.
- [29] Cargnoni F, Nishibori E, Rabiller P, Bertini L, Snyder GJ, Christensen M, et al. *Chem Eur J* 2004;10:3861–70.